

# Demonstrations of Multi-Constellation Advanced RAIM for Vertical Guidance using GPS and GLONASS Signals

Myungjun Choi, Juan Blanch, *Stanford University*  
Dennis Akos, *University of Colorado Boulder*  
Liang Heng, Grace Gao, Todd Walter, Per Enge. *Stanford University*

## ABSTRACT

In the near future, many more navigation satellites with dual frequency L1 and L5 will be deployed. The increased number of satellites and the possibility of mitigating the ionospheric delay using dual frequency have opened the door to the possible use of RAIM for vertical guidance. For this purpose, several Advanced RAIM (ARAIM) algorithms have been proposed. Extensive simulation studies have established that with two constellations it might be possible to achieve global coverage of LPV 200, which requires a 35 meter Vertical Alert Limit. Previous work [1], [2], [3] with large amounts of receiver data has demonstrated the ability of ARAIM to compute a Vertical Protection Level (VPL) that bounds the Vertical Position Error (VPE). However, in that effort, only GPS measurements were tested for the validation of ARAIM. Therefore, multi-constellation evaluation of ARAIM performance will be necessary. In addition to GPS, the only full constellation, or nearing Final Operation Capability, is GLONASS.

In this paper, we will validate ARAIM further using ten days of GPS and GLONASS measurements collected by a GLONASS capable GNSS receiver. From the stored data, we will compute all the figures of merit that are necessary for LPV-200, in particular the Vertical Protection Level (VPL) and the accuracy. We will test the ability of the algorithm to predict accuracy and its ability to compute a VPL that bounds the Vertical Protection Error. This will represent one of the first demonstrations of multi-constellation ARAIM with real data.

## INTRODUCTION

The GNSS environment is being enhanced in two ways. First, as a part of GPS modernization, an additional signal in the L5 frequency band will be transmitted. Second, new GNSS constellations, such as GLONASS, Galileo,

and Compass, have been launched and they are currently being built or replenished. We can take advantage of these two enhancements for civil aviation. Combining the L1 frequency and new L5 signal, we can eliminate the error due to the ionospheric delay. In addition, more ranging sources will increase the redundancy to the point where eventually they may be used for vertical guidance through ARAIM in civil aviation safety. Previous work [3], [4], [5], [6], [7] has examined the possibility of achieving global coverage of LPV 200. In addition, in previous studies, the basics of an ARAIM prototype have been proposed [8] and the algorithm has been tested with flight test data [2]. Moreover, a demonstration using extensive GPS real ground data has shown the ability of ARAIM to effectively bound the Vertical Position Error [1]. The purpose of this paper is to extend the work of [1] to a multi-constellation setting by using GPS and GLONASS real data. This will represent one of the first demonstrations of multi-constellation ARAIM with real data.

This paper is presented as follows. First, the data collection details are presented. This explains how the GPS and GLONASS real measurement data and navigation messages were obtained from the receiver, and how they were processed. Then, the ARAIM evaluation tool is described, as well as multipath error model. Next we evaluate the algorithm. The first part consists of checking that the nominal error models are correct. We do this by evaluating whether predicted position accuracy is well fitted to the position solution with given measurements and error model. Then, the VPL bounding performance is analyzed under nominal conditions and one satellite failed condition. Finally, the availability is assessed.

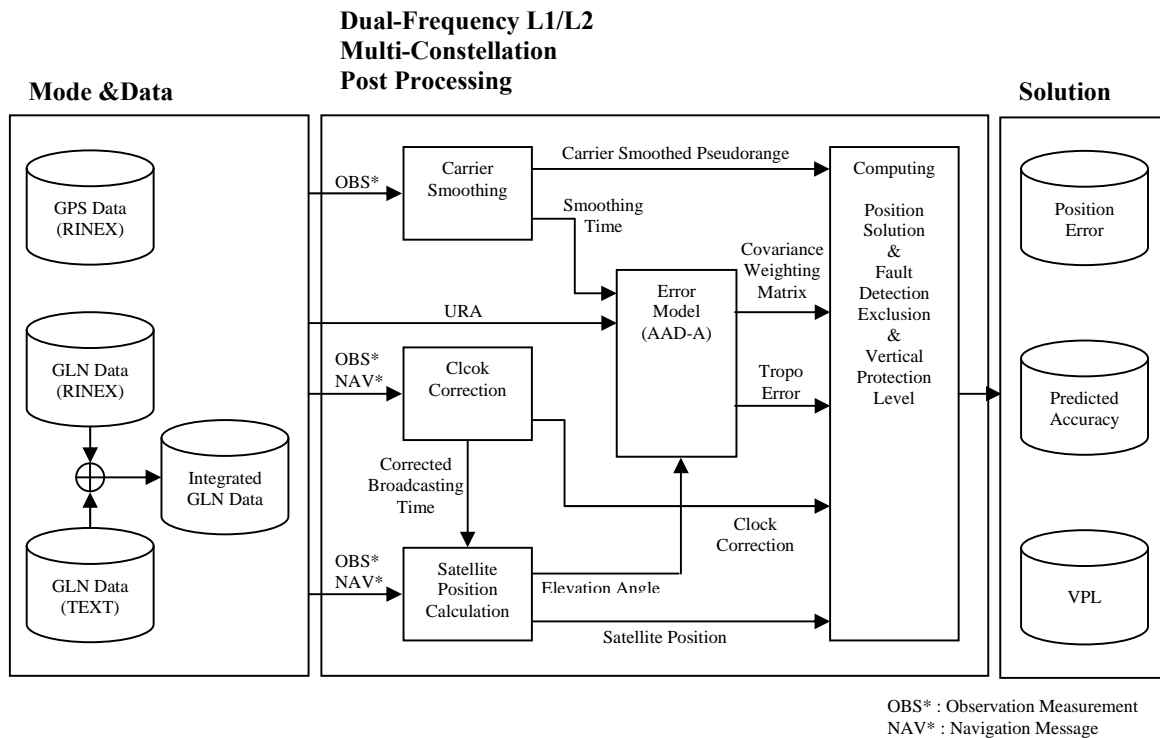


*Figure 1. ARAIM Evaluation Tool Block Diagram*

## DATA COLLECTION

This section describes the source of the data and the multi-constellation ARAIM algorithm processing. The data was obtained from a multi-constellation capable receiver installed whose antenna is on the roof of the Stanford GPS laboratory. Since the receiver was installed, we have stored all navigation messages and measurement data that can be tracked by the receiver. Since the receiver can be connected via TCP/IP, we are able to monitor in real time the satellite tracking and log the stored data. When the receiver gets the data, it saves it as a \*.T02 file format. Users can then access the data on the intranet. However, the storage volume is not enough to save all the data for several months, so we established a system that transmits the data into the server computer in the laboratory. The \*.T02 file format is an assembled data format which is comprised of GPS, GLONASS, Galileo, and WAAS data. Hence it is necessary to convert it into a more convenient file format for post processing. With the conversion tool, we can convert the \*.T02 file into a GPS or GLONASS RINEX file. In addition, it is also necessary to parse the \*.T02 file into a text file with the GLONASS navigation message, because the GLONASS RINEX files do not contain the URA and  $\tau$ GPS.  $\tau$ GPS is the time difference between GLONASS time scale and GPS time scale, and is needed to synchronize GPS and GLONASS. The URA is necessary to compute the pseudorange error model which will be applied to form the weighting matrix for the position solution

computation. Through these procedure, we processed 10 days of GPS and GLONASS data from 6/1/2011 to 6/10/2011 collected at Stanford University.

## ARAIM EVALUATION TOOL

The ARAIM evaluation tool has the capability to compute the position solution as well as the VPL which bounds the VPE. The evaluation tool consists of three modules as described in Figure 1. They are mode and data selector, post processing, and solution record module. Since we have two constellations' worth of data, three combination modes can be chosen by users, which are GPS only, GLONASS only, or integrated GPS and GLONASS mode. If the mode is selected by the user, the data management component loads the available data set and distributes the post processing module.

With the navigation message and the observation measurement, satellite clock bias and satellite position are computed in the corresponding component, respectively. Carrier smoothing is also implemented for the next process which is position computing. In this component, ionosphere-free combinations are used both for code and carrier inputs to the smoothing filter in order to remove ionospheric delay. In addition, the carrier smoothing component not only sets the smoothing time filter to 200 s, but also records each satellite measurement's smoothing time in order to characterize range error

model. Then, the output, satellite elevation angle and smoothing time from previous components and the URA, which is one of the elements in the navigation message, are transferred into the error model component. In the error model component, the total variance that contains multipath, receiver noise, and tropospheric error model is calculated to produce the weighting matrix for the weighted least square solution in position computing. Finally, the ARAIM tool calculates position solution. After that, it checks to see if the satellite is faulty, and excludes the corresponding measurement. If the fault detection test is passed as described in [1], the tool computes the real time VPL. Lastly, if the process is over solution record module saves all the result data.

### Range Error Model

The range error model component plays an important role in this work, specifically it characterizes one aspect of ARAIM algorithm ability which is predicting accuracy. As noted in [8], the ARAIM algorithm will be implemented in an airborne situation. Hence, we used the error model of an airborne receiver, even though we collected real data through a ground receiver. We call that nominal error model Airborne Accuracy Designators (AAD-A). The following equations specify this model.

The total variance is defined as:

$$\sigma_k^2 = \sigma_{k,URA}^2 + \sigma_{k,tropo}^2 + \sigma_{k,DF\_air}^2 \quad (1)$$

Where:

The tropospheric error is defined as:

$$\sigma_{k,tropo} = (0.12 \text{ m}) \cdot \left( \frac{1.001}{\sqrt{0.002001 + \sin^2(EI_k)}} \right) \quad (2)$$

The CNMP error is modeled as:

$$\sigma_{k,DF\_air}^2 = \left( \frac{f_1^2}{f_1^2 - f_2^2} \right) \sigma_{L1,k,air}^2 + \left( \frac{f_2^2}{f_1^2 - f_2^2} \right) \sigma_{L2,k,air}^2 \quad (3)$$

$$\sigma_{L1,k,air}^2 = \sigma_{L2,k,air}^2 = \sigma_{k,noise}^2 + \sigma_{k,multipath}^2 \quad (4)$$

$f_1$  and  $f_2$  are the L1 and L2 frequencies.

The noise term is specified in the following:

$$\sigma_{k,noise} = 0.04 \text{ m} - (0.02 \text{ m})(\theta_k - 5^\circ) / (85^\circ) \quad (5)$$

The multipath error model is followed as:

$$\sigma_{k,multipath} = \alpha \times (0.13 + 0.53 \times e^{-\theta_k/10^\circ}) \quad (6)$$

Unlike previous work [1], we appended additional term  $\alpha$  which is the multiplication factor in Equation (6). The coefficient  $\alpha$  is a function of carrier smoothing time of the measurement and is inversely proportional to the square root of smoothing time. Therefore, as smoothing time increases, the coefficient decreases and converges to one. We set the convergence point as 30 s. By applying the adjusted multipath error model, we tried to generate well estimated predicted accuracy. Since the tropospheric term is independent of both receiver noise and multipath, and URA is the constant value we can receive from the navigation message, the multipath error model has been modified.

**Table 1.** Comparison of GPS and GLONASS

Parameter	GPS	GLONASS
Time Scale	UTC(USNO)	UTC(SU)
Reference Coordinate	WGS-84	PZ-90
Carrier Frequency	L1:1602.0+0.5625k L2:1246.9+0.4375k k = 0,1...12	L1:1575.42 L2:1227.6
Ephemeris	Keplerian elements	Rectangular Coordinates

### GLONASS only mode

Since the GLONASS satellite transmits different navigation messages than GPS, GLONASS has another scheme to calculate satellite clock bias and satellite position based on GLONASS ICD [9]. Also several considerations are required to get a position solution using GLONASS signals. First, since each GLONASS satellite transmits respective carrier frequency, the available frequency value should be reflected in the computing error model, such as Equation (3), and carrier smoothing as described in Table 1. Next, considering Earth's rotation rate and the time difference between the instant in time of signal reception and the time of signal transmission, there is a common bias term in the east component of position error in the process of verification of our tool. Because the factor that causes common bias is not known even after careful analysis, we characterized the bias term in the position domain and tracked back errors in the range domain. We then subtracted range domain errors from the measurements and computed the position solution again. Other issues such as time scale and reference coordinate system will be presented in the following paragraph.

## Combining GPS and GLONASS

One of the key features in this paper is to compare the performance between single constellation mode and multi-constellation mode. As a result, in integrated GPS and GLONASS mode, the different reference parameters should be synchronized with one reference frame for exact comparison. Table 1 presents key parameters that should be considered in combining GPS and GLONASS signals. In this work, since every signal is measured based on the GPS time standard in the receiver, all the reference parameters were matched up with GPS. Thus, for time scale, originally GLONASS time should have been corrected in four ways: constant three hour difference between GLONASS and UTC(SU) time scale, UTC(SU) correction,  $\tau_{GPS}$ , and leap seconds based on GLONASS ICD [10]. However, since the receiver provides all time scales associated with GLONASS with the UTC(SU) time scale, and the UTC(SU) correction is sufficiently small to ignore, we applied  $\tau_{GPS}$  and leap seconds to time data associated with GLONASS. For the reference coordinate system, GPS uses WGS-84 and GLONASS uses PZ-90 as shown in Table 1. Hence, the transformation matrix for converting PZ-90 to WGS-84 has to be applied after calculating the GLONASS satellite position. In combining geometries and time in a matrix for the weighted least square solution, the geometric matrix is given by

$$G = \begin{bmatrix} \alpha_x^{gps1} & \alpha_y^{gps1} & \alpha_z^{gps1} & 1 & 0 \\ \vdots & \vdots & \vdots & \vdots & \vdots \\ \alpha_x^{gpsN} & \alpha_y^{gpsN} & \alpha_z^{gpsN} & 1 & 0 \\ \alpha_x^{gln1} & \alpha_y^{gln1} & \alpha_z^{gln1} & 0 & 1 \\ \vdots & \vdots & \vdots & \vdots & \vdots \\ \alpha_x^{glnM} & \alpha_y^{glnM} & \alpha_z^{glnM} & 0 & 1 \end{bmatrix} \quad (7)$$

Zeros and ones for clock bias in a matrix should be located in a different column in order to get each receiver

clock bias, because the receiver clock offset for GPS and GLONASS is different.

Through this data collection and processing set up, we can verify two competencies of ARAIM in the following section.

## RESULT 1 : Predicted Accuracy Analysis

Figure 2 shows the VPE histogram of each mode for 10 days. In GPS only mode, the standard deviation is close to the value in the GPS PAN Report in northern California, while GLONASS only mode produces the large error and standard deviation. However, the standard deviation of GPS + GLONASS mode is relatively greater than the one of GPS only mode. By examining GLONASS only mode performance, we could infer that the unpleasantly predicted GLONASS error model affected the result of position error in combined mode. The reason for this is because when we applied the weight of GLONASS measurements to the weighted least square solution, the error model, specifically multipath model, had lower value than it otherwise would have. Detailed information about this will be presented with the predicted accuracy representation.

Since we had enough sample results, the performance of range error characterization, which is one aspect of ARAIM ability, can be evaluated. The predicted accuracy is a function of geometries and error model statistics before the tool gets a position solution in every epoch. Comparing predicted accuracy and experimental result for position error, we can verify whether or not the tool predicts accuracy effectively. Thus we divide the VPE by the predicted accuracy in order to show that the resulting distribution is close to a standard normal distribution. If so, we can say the tool is able to produce a good error model.

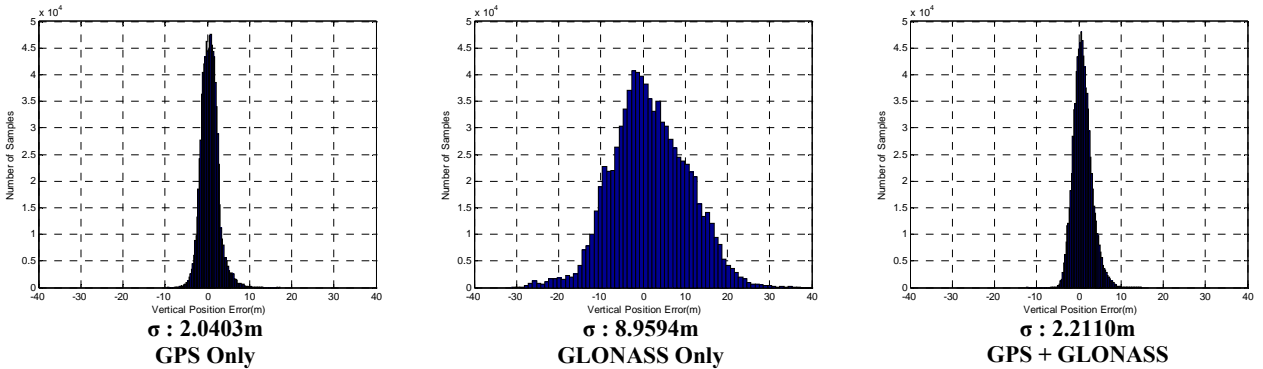
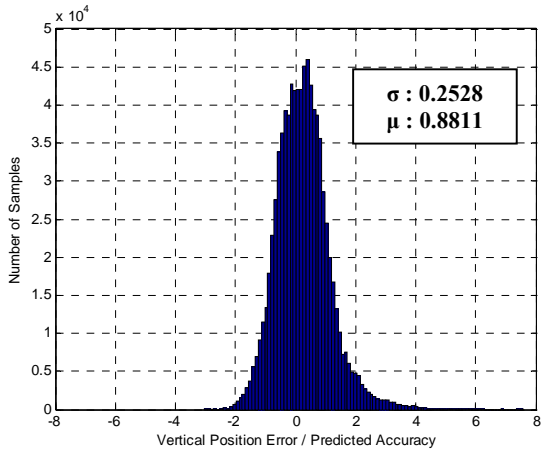
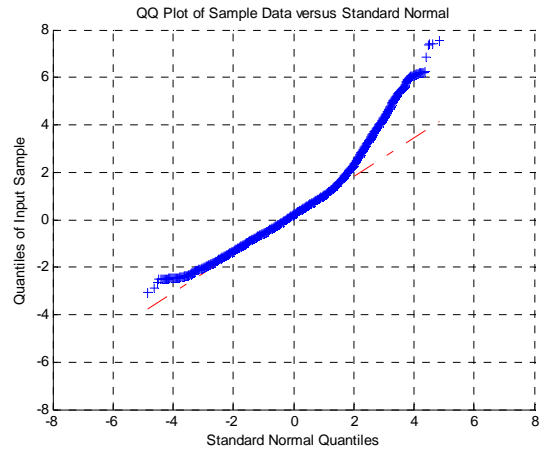


Figure 2. Vertical Position Error Histogram

**GPS Only**

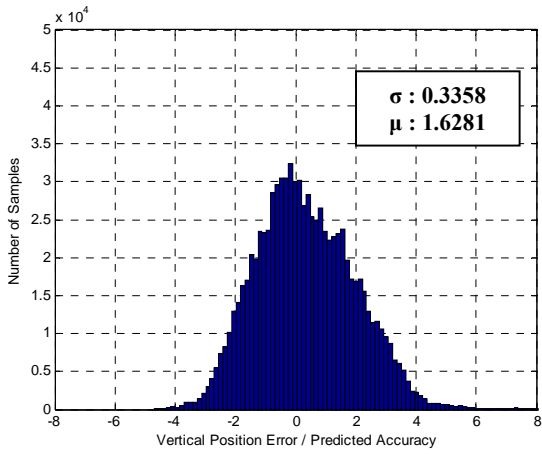


(a)

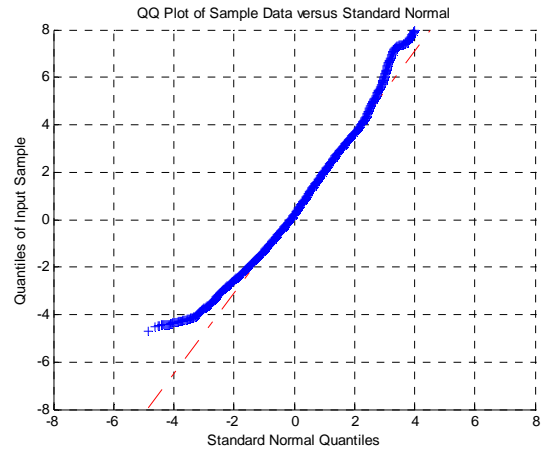


(b)

**GLONASS Only**

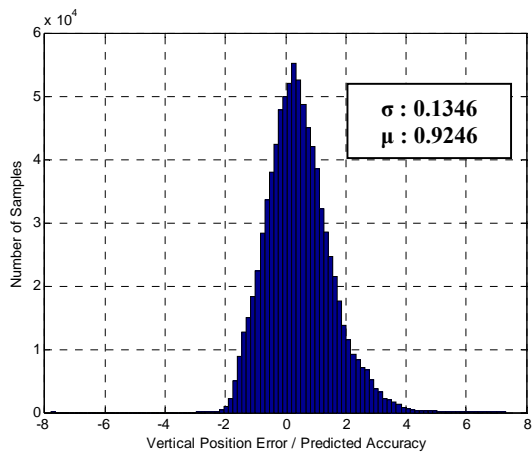


(c)

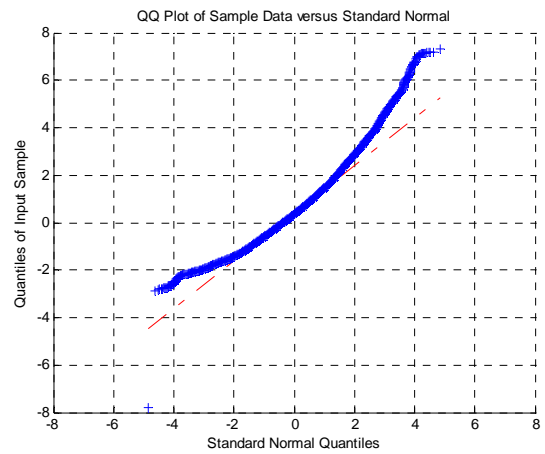


(d)

**GPS + GLONASS**



(e)



(f)

**Figure 3. Normalized VPE Distribution Histogram and Quantile Quantile Plot**

Figure 3 presents the result distribution and quantile representation of each mode concerning prediction ability of the tool. Figure 3(a) shows the histogram of the normalized position error for GPS only mode. As the mean value and standard deviation of the histogram shows, the position error normalized to the predicted accuracy is more likely to be a standard normal distribution. Figures 3(b), (d), and (f) are the quantile plots (q-q plot) which display the quantitative relationship between sample result quantiles of the normalized VPE and theoretical quantiles from a normal distribution. If the distribution of the former is normal, the plot will be close to linear. According to the histogram of the GPS only mode, the corresponding q-q plot, Figure 3(b), is almost a linear line except outside the interval ranging from -2 to 2. That means even the histogram approximately looks like a standard normal distribution, though specifically there are some measurements whose range error statistics are not predicted well. Figures 3(c) and (d) are the GLONASS only mode results. From these, we can infer easily that the algorithm did not predict range error well. Even though there is the adverse affect of the GLONASS portion of the solution, the combined mode provides a positive outcome as you see in Figures 3(e) and (f). Meanwhile, since the weighting matrix for the position solution is dependent on the range error model which also affects the predicted accuracy, poor prediction against GLONASS measurement is related to the inaccurate weighting matrix so that the accuracy of combined mode is greater than that of the GPS single mode. Therefore, it is necessary to design an accurate multipath model according to the range error model paragraph. Most importantly, the multipath coefficient curve takes on the same value as in the GPS case, so that a feasible respective error model is required for each constellation.

## RESULT 2 : VPL Bounding

### *Behavior under the Nominal Condition*

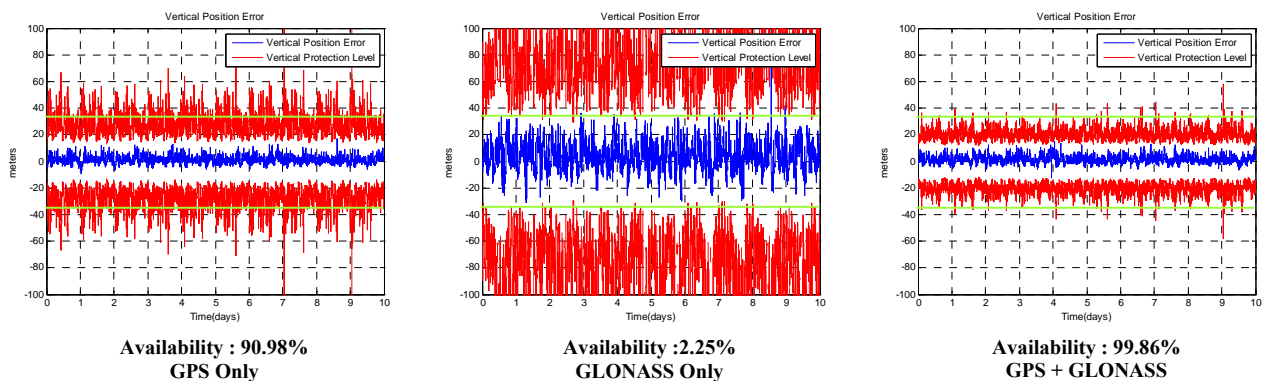


**Figure 4.** VPE and VPL under the nominal condition

Another significant aspect of ARAIM evaluation is whether or not the VPL bounds the VPE during navigation operation, because VPL, which is the estimated vertical error bound, is related to the requirements in aviation navigation safety, such as integrity and availability. Hence, if there is a situation in which the VPL does not bound the VPE, users will not be able to obtain necessary aviation operation levels for safety. Furthermore, a larger number of values of VPL below certain Vertical Alert Limits (VAL) during aviation would increase the availability of the system. Figure 4 displays the Vertical Position Error and the Vertical Protection Level for 10 days from June 1<sup>st</sup> to June 10<sup>th</sup>, 2011 at Stanford University. Under the producing 100% position solution of each mode, the algorithm generates the VPL which always bounds the VPL. However, the position solution often carries noise. The reason each mode has noise in the position solution is because we used code phase rather than carrier phase. In the process of converting \*.T02 file format into the corresponding RINEX observation file, we discovered non-available carrier phase data. This situation happened many times even though code phase data had existed without problem. This had an effect on the reset of the carrier smoothing filter and, it turns out, on the noisy position solution. The positive side is the dramatic change of the decreased value of the VPL in combined mode compared to any other single constellation mode. The green horizontal line on each plot is the VAL which is equal to 35 m. This specific value is the requirement of LPV 200. There are many cases in which the value of the VPL is less than the VAL, 35 m in combined mode. If we calculate the percentage of time that the VPL is less than 35 m out of total epochs, which is the availability, GPS only mode is 90.98% and GLONASS only mode is 2.25%. Lastly, combined GPS and GLONASS mode has the value of 99.86%, which meets the requirement of LPV 200.

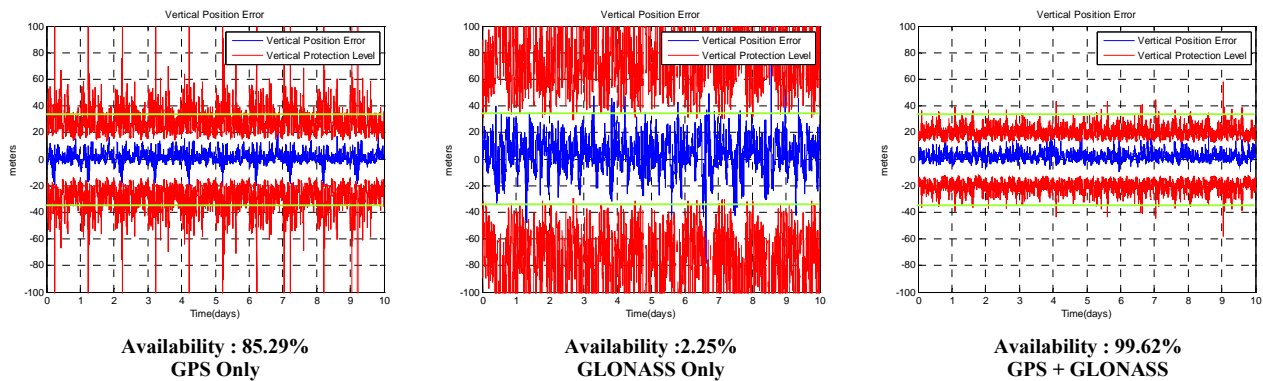


**Figure 5.** VPE and VPL under the one injected failure

### Behavior under the one injected failure

In this case, we inserted a 20 m bias deliberately on all measurements of one specific satellite at all times in order to examine how our results changed in a fault situation. For GPS and GLONASS combined mode, I did not select respective satellites among each constellation, but select one specific GPS satellite. Figure 5 shows the VPE and the VPL under one injected failure for the same days as in the previous paragraph. Due to failure, the bias position error and the VPL have been increased. However, even if the fault is undetected, the VPL is always greater than the VPE. Also, even though the availability of GPS only and combined mode is reduced a little bit, it still sustains higher availability, and GLONASS only mode does not show any change.

### CONCLUSION

The proposed ARAIM prototype from [8] could have been examined in different ways than the previous extensive validation [1]. In this study we conducted tests with extended constellations, i.e., GPS and GLONASS, through a GNSS receiver which can track multi-constellations. Similar to the previous work [1], we calculated the VPEs and the VPLs using the ARAIM Evaluation tool for 10 days using both single constellation and multi-constellation configurations. In addition, we verified two aspects of ARAIM capability: the predicting accuracy ability and the VPL bounding. The algorithm computes position 100% in any mode and we observed in all situations that the VPE was less than the VPL as we expected. Even under the fault condition, the algorithm performs well showing robust error bounding. However, error model estimation performance depends on the constellation and it is necessary to design a reliable error model in order to provide better accuracy prediction.

Eventually, more ranging sources from multi-constellation will guarantee narrower error bounding than single constellation and under the assumptions used here, multi-constellation ARAIM meets the requirements for LPV-200.

A subsequent work is composed of reconstructing missing L1/L2 code in the \*.T02 file and designing a more capable multipath error model. Moreover, we will test with extended failure states such as multiple satellites and constellation failure. Lastly, we will stretch out our study to other requirements of ARAIM with multi-constellation in order to increase the possible use of ARAIM in aviation safety.

### ACKNOWLEDGEMENTS

The authors gratefully acknowledge the Federal Aviation Administration (FAA) grant CRDA 08-G-007 for supporting this. The opinions discussed here are those of the authors and do not necessarily represent those of the FAA or other affiliated agencies.

### REFERENCES

- [1] M. Choi *et al.* "Advanced RAIM Demonstration using Four Months of Ground Data" *Proceedings of ION ITM 2011*, San Diego, CA, 2011.
- [2] A. Ene *et al.* "Validation of Multiple Hypothesis RAIM Algorithm using Dual-Frequency GPS and Galileo Signals." *Proceedings of the European Navigation Conference GNSS 2008*, Toulouse, France.

[3] *GNSS Evolutionary Architecture Study Phase II Report.*

[http://www.faa.gov/about/office\\_org/headquarters\\_offices/ato/service\\_units/techops/navservices/gnss/library/documents/](http://www.faa.gov/about/office_org/headquarters_offices/ato/service_units/techops/navservices/gnss/library/documents/)

[4] T. Walter *et al.* "Worldwide Vertical Guidance of Aircraft Based on Modernized GPS and New Integrity Augmentations." *Proceedings of the IEEE Special Issue on Aviation Information Systems*. Vol. 96 Nr. 12, December 2008.

[5] J. Blanch *et al.* "RAIM with Optimal Integrity and Continuity Allocations Under Multiple Satellite Failures." *IEEE Transactions on Aerospace Electronics*. Vol. 46, Nr 3, July 2010.

[6] Y.C. Lee *et al.* "Analysis of RAIM Using Multi-Constellation To Provide LPV-200 Service Worldwide." *Proceedings of the ION GNSS 2010*, Portland, 2010.

[7] A. Ene. "Further Development of Galileo-GPS RAIM for Vertical Guidance." *Proceedings of the ION GNSS 06*, Fort Worth, 2006.

[8] J. Blanch *et al.* "Prototyping Advanced RAIM for vertical guidance", *Proceedings of ION GNSS 2010*, Portland, OR, 2010.

[9] *GLONASS Interface Control Document.*

<http://gauss.gge.unb.ca/>